Modelling the Subsurface Geomorphology of an Active Landslide Using LIDAR

by

Norbert Maerz

NUTC
R331

Disclaimer

The contents of this report reflect the views of the author(s), who are responsible for the facts and the accuracy of information presented herein. This document is disseminated under the sponsorship of the Department of Transportation, University Transportation Centers Program and the Center for Transportation Infrastructure and Safety NUTC program at the Missouri University of Science and Technology, in the interest of information exchange. The U.S. Government and Center for Transportation Infrastructure and Safety assumes no liability for the contents or use thereof.

Technical Report Documentation Page

1. Report No. NUTC R331	2. Government Accession No.	3. Recipient's Catalog No.
4. Title and Subtitle Modelling the Subsurface Geomorphology of an Active Landslide Using LIDAR	5. Report Date July 2014	
	6. Performing Organization Code	
7. Author/s Norbert Maerz	8. Performing Organization Report No. Project #00042038	
9. Performing Organization Name and Address Center for Transportation Infrastructure and Safety/NUTC program Missouri University of Science and Technology 220 Engineering Research Lab Rolla, MO 65409	10. Work Unit No. (TRAIS)	
	11. Contract or Grant No. DTRT06-G-0014	
12. Sponsoring Organization Name and Address U.S. Department of Transportation Research and Innovative Technology Administration 1200 New Jersey Avenue, SE Washington, DC 20590	13. Type of Report and Period Covered Final	
	14. Sponsoring Agency Code	
15. Supplementary Notes		

16. Abstract

The focus of this research was twofold:
1. To determine millimeter/sub-millimeter movement within a slide body using high precision terrestrial LIDAR and artificial targets. This allows movement not apparent to the naked eye to be verified.
2. To quickly and easily determine the depth of the shear surface using high precision terrestrial LIDAR and artificial targets. This would allow rotational measurements.

To do this, 5/8" steel reinforcing rods were cut in lengths of 3, 4, and 5'. These rods were driven into the ground to various depths. 4" precision Styrofoam balls were mounted onto the rods. Using LIDAR scanning, the displacement of the styrofoam balls (in successive LIDAR scans) can be measured to within 0.9 mm. This allows the sub-millimeter displacement (objective 1) to be measured. Furthermore, when two of the Styrofoam balls are placed on a rod, not only the movement, but also the rotation of the rod, and consequently the precise movement of the ground the rod is in can be measured. Figure 1 shows a 5/8" rebar with two Styrofoam balls driven into the ground.

17. Key Words Rock fall, land slide, LIDAR	18. Distribution Statement No restrictions. This document is available to the public through the National Technical Information Service, Springfield, Virginia 22161.		
19. Security Classification (of this report) unclassified	20. Security Classification (of this page) unclassified	21. No. Of Pages 15	22. Price

Form DOT F 1700.7 (8-72)

Modelling the Subsurface Geomorphology of an Active Landslide Using LIDAR

1. Background

Soft slope movement is a big problem whether it involves an engineered slope or one that is near infrastructure, or both. Active landslides often fail slowly, so there is sometime ample time to affect remedial works. In order to effectively plan remedial works, we must be able to model the entire geometry of the slide. Unlike the surface geometry, which can be easily discerned, the below grade geometry is both critical and difficult (if not impossible to map). The failure surface could be planar, circular, or follow a composite path. It could be shallow or deep. There could be a single failure surface, or the slide could be composed of multiple failure surfaces. Different failure surfaces require different methods of analysis and different remediation/mitigation options.

Traditionally engineers have made assumptions about the failure surface, or assumed that the failure surface occurs along a path of maximum shear stress Sometimes the geology below the slide is determined by expensive and time consuming drilling, and the geological knowledge is used to guide the analysis. Even then the drilling can show zones of weakness, but typically does not identify the shear surface.

To uniquely identify the failure surface requires the installation of inclinometers in boreholes. This is an extremely costly enterprise, especially where composite surfaces are involved.

2. Principal of the New Approach

The focus of this research was twofold:

1. To determine millimeter/sub-millimeter movement within a slide body using high precision terrestrial LIDAR and artificial targets. This allows movement not apparent to the naked eye to be verified.
2. To quickly and easily determine the depth of the shear surface using high precision terrestrial LIDAR and artificial targets. This would allow rotational measurements.

To do this, 5/8" steel reinforcing rods were cut in lengths of 3, 4, and 5'. These rods were driven into the ground to various depths. 4" precision Styrofoam balls were mounted onto the rods. Using LIDAR scanning, the displacement of the styrofoam balls (in successive LIDAR scans) can be measured to within 0.9 mm. This allows the sub-millimeter displacement (objective 1) to be measured. Furthermore, when two of the Styrofoam balls are placed on a rod, not only the movement, but also the rotation of the rod, and consequently the precise movement of the ground the rod is in can be measured. Figure 1 shows a 5/8" rebar with two Styrofoam balls driven into the ground.

Figure 1: 5/8" rebar driven into the ground with two styrofoam balls.	Figure 2: Movement of styrofoam balls above a planar shear surface, when the base of the rod is above the shear surface.
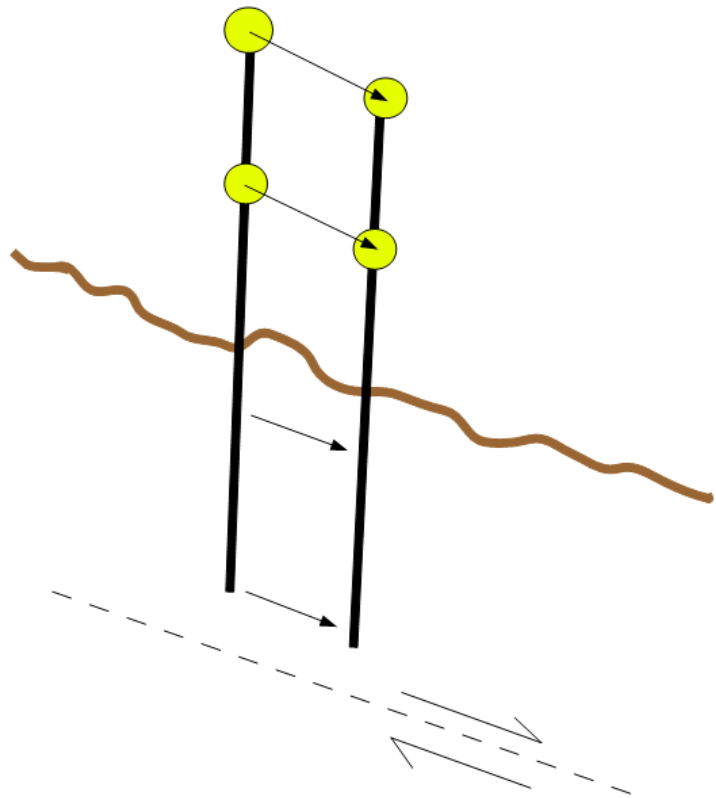
Figure 2 shows the relative movement of the rod and styrofoam balls when the base of the rod is above a planar shear surface. Figure 3 shows the relative movement of the rod and styrofoam balls when the base of the rod is below a planar shear surface. Figure 3 shows the relative movement of the rod and styrofoam balls when the base of the rod is above a shear circular shear surface.

In this way, be measuring the relative movement of the balls between successive LDAR scans, the magnitude, direction, and rotation of the ground can be accurately determined.

Using many rods positioned in different locations and driven into the ground to different depths, the geomorphology of the failure surface can be determined as well as the rate and direction of advance of the slide. The cost of each addition rod only adds incrementally small cost to the project.

Figure 3: Movement of styrofoam balls above a planar shear surface, when the base of the rod is below the shear surface.

Figure 4: Movement of styrofoam balls above a circular shear surface, when the base of the rod is about the shear surface.
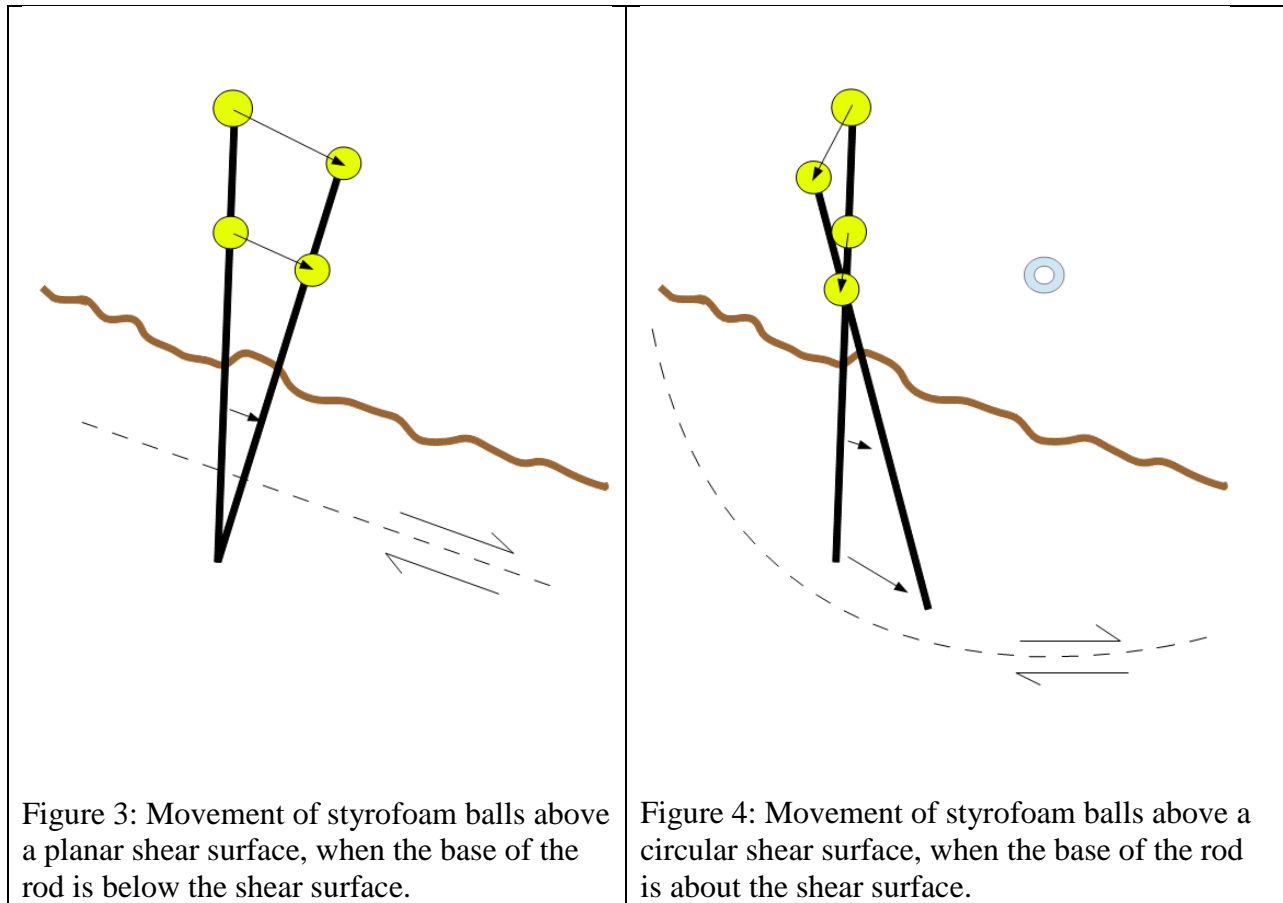
3. Simulated Measurements on a Small Embankment

For this test, a small embankment was used. (This embankment did not show any signs of earth movement). Six rods were driven into the ground to a depth of about 2.5' (Figure 5). Two of the rods were 4' long and had a single ball mounted on the rod. Three of the rods were 5' long and had a dual ball mounted on the rod. These were the measurement rods.

After installation, a LIDAR scan was conducted (Figure 6). Then, to simulate earth movement, three of the rods were manually pushed forward about 2". A second LIDAR scan was performed after this. The two LIDAR scan point clouds were registered to each other using the balls that were not manually moved.

Finally the positional differences of the balls were calculated and displayed (Figure 7). Movement of 68.5 and 72.7 mm were measured. The error (as measured by the relative positions of the stationary balls) was found to be about 1 mm.

Figure 5: Embankment with six rods driven in 2.5' deep. The rods with single balls were 4' log and the rods with multiple balls are 5' long.
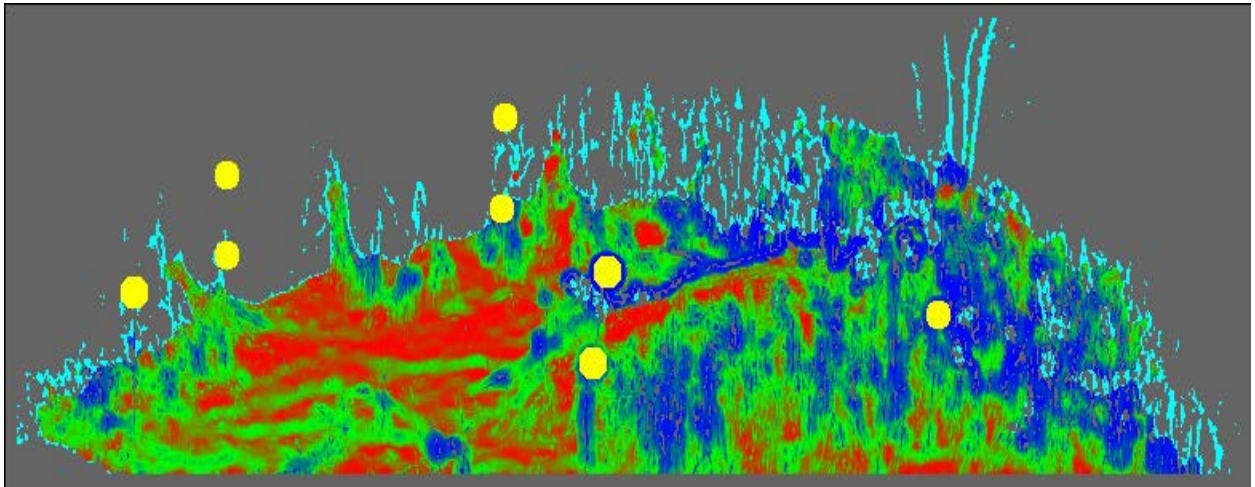
Figure 6: LIDAR Scan of the scene of Figure 5.
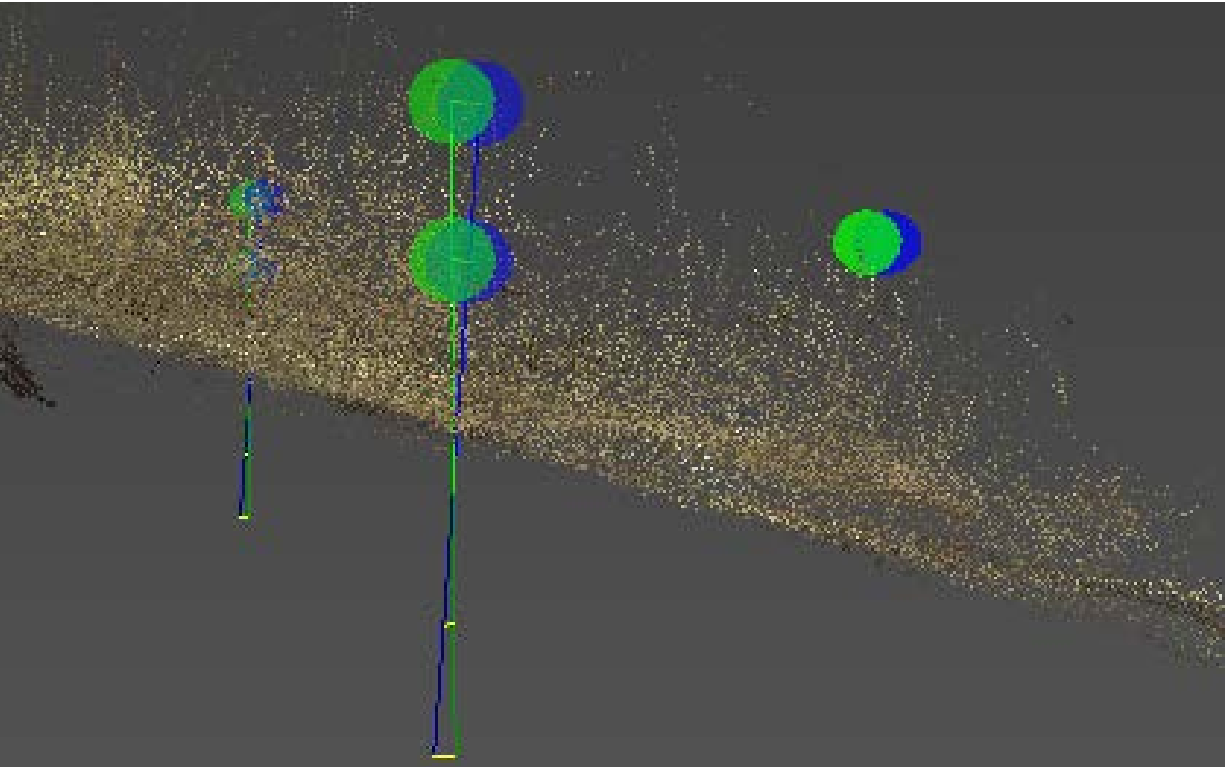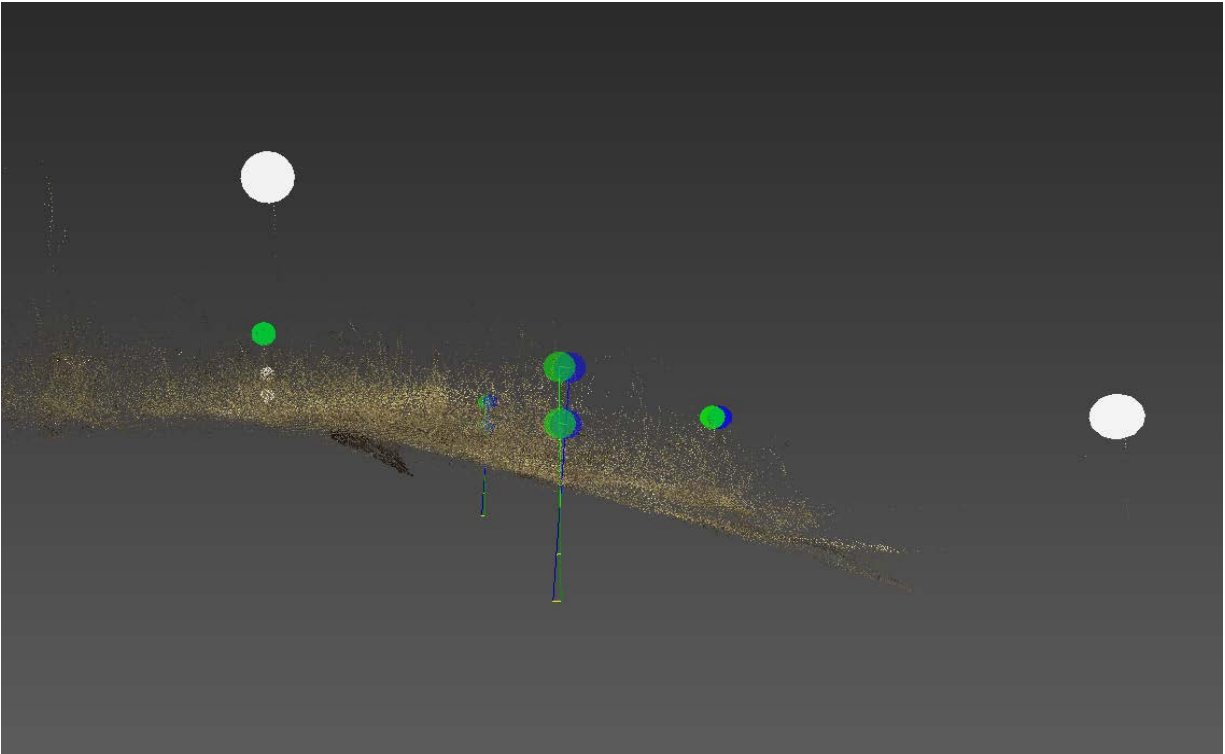
Figure 7: Example of movement of rods and balls. The white balls served as control, the blue rods and balls represent the "before" configuration, and the green rods and balls represent the "after" configuration. Displacement vectors are shown in yellow.

4. Processing Procedure

A rod configuration file is created which defines the purpose and configuration of each rod. Each line in this file describes a rod, its type (control or floating), the bottom ball ID, top ball ID, and the rod length in feet.

Example of rodConfig.txt file:

```
c 1 1 4
c 2 2 4
f 4 3 5
f 6 6 4
f 5 5 4
f 8 7 5
c 10 9 4
```

In this example, 7 rods were defined - three control rods, and four floating rods. Rods with the same ball ID for top and bottom represent rods with only one ball attached. The balls on the control rods will be used to calculate a 7-parameter 3-D conformal transformation. The balls on the floating rods will be transformed to the coordinate system defined during the base-date scan.

Next, the balls are manually assigned ID's using an application which displays the LIDAR scene as a depth image (Figure 8) Each ball is identified with a role (control or float) and a numeric ball ID. The manual pointings do not have to be precise - any location within a ball radius will serve the purpose.

Next, a program is run to compute the theoretical sphere center for each ball. The method uses the manual pointings to define a search zone around each ball. The original LIDAR point cloud
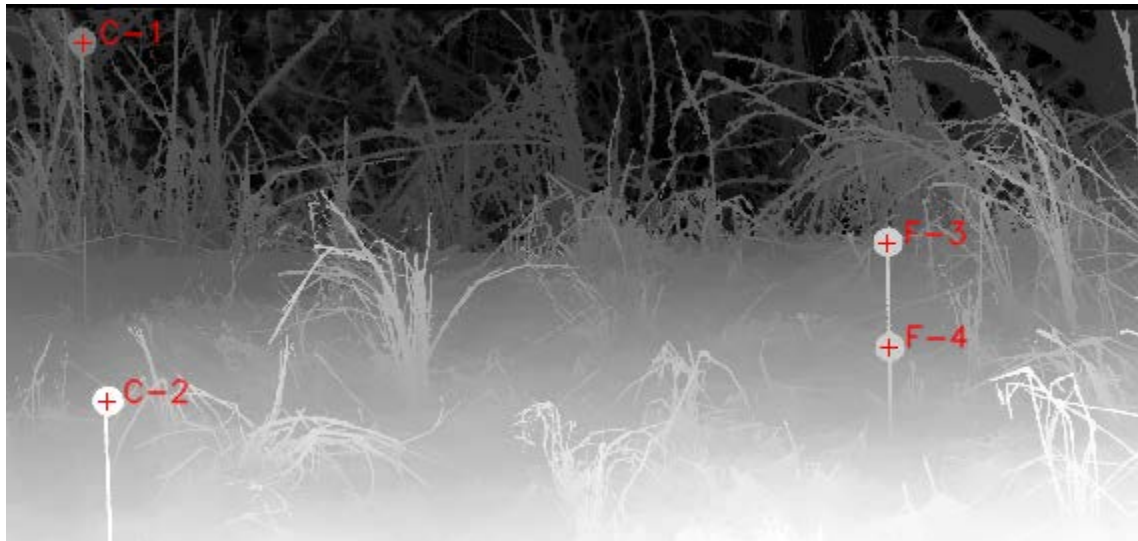
Figure 8: Identification of the rods and balls.

data is used to collect candidate points which fit a hemispherical template defined for the search zone. Typically, 2000 - 4000 raw LIDAR points are collected for each ball - representing the surface hemisphere of the ball visible to the LIDAR. Next, a recursive algorithm is executed on this set of surface points to determine the theoretical center of the spherical target. The recursion continues until the refined center position converges to less than 0.001 mm per cycle. The resultant theoretical center is the point which minimizes the standard deviation of all the radial surface observations (distances from the theoretical center to each LIDAR surface observation). The precision of the sphere centers is less than 0.1 mm for 4" target balls imaged at 180 feet, using 1mm scanning resolution and approximately 2000 surface observations per ball.

Finally, using information in the rodConfig file, a model of each rod / ball combination is created. The position and orientation of each rod is computed by assuming the rod remained rigid, and projecting the rod dimensions using the precise locations of the balls located on the upper part of each rod. Using this method, the subterranean position and orientation of each rod can be established. Finally, displacement vectors are generated for five points along each rod - at the two ball positions, at ground level, and at two subterranean positions.   The modeled rods and the original LIDAR point cloud data are used to create a 3-D VRML (Virtual Reality Modeling Language) model, which can be viewed in any browser having a free VRML plug-in.

In this view (Figure 7), the white balls served as control, the blue rods and balls represent the "before" configuration, and the green rods and balls represent the "after" configuration. Displacement vectors are shown in yellow. The bright part of each rod is that portion above ground level - the subterranean segment of each rod is shown in a darker shade of blue or green. Only rods with two balls are shown with modeled rods and their respective displacements.

5. Measurements on a Landslide on Highway 65 near Branson MO

An active landslide near Branson MO (Highway 65) was selected to verify the principle. The goal of the study is to model how a landslide deforms over time. Figure 9 shows the roadside slope. A head scarp is obvious at the top of the slope, and the sides of the slide are well defined. Figure 8 also shows the planned locations of control points and measuring points.

Using different lengths of rebar (3, 4, and 5 feet) and 4 inch Styrofoam balls placed in a network over the slide body (Figure 9). A total of 54 pieces of rebar with two balls each were placed over the slide. An additional 6 pieces of rebar with one ball apiece will be used as control points and therefore placed outside of the movement area.

To date, 2 LIDAR scans have been taken, one on March 26 and another on May 21.

Figure 9: Landslide on Highway 65 in Branson, Stone County. The yellow stars indicated planned control bars and balls, and the intersection points of the red grid represent planned measuring points. Top image from Google Earth.

Figure 10: Final layout of the rods and balls
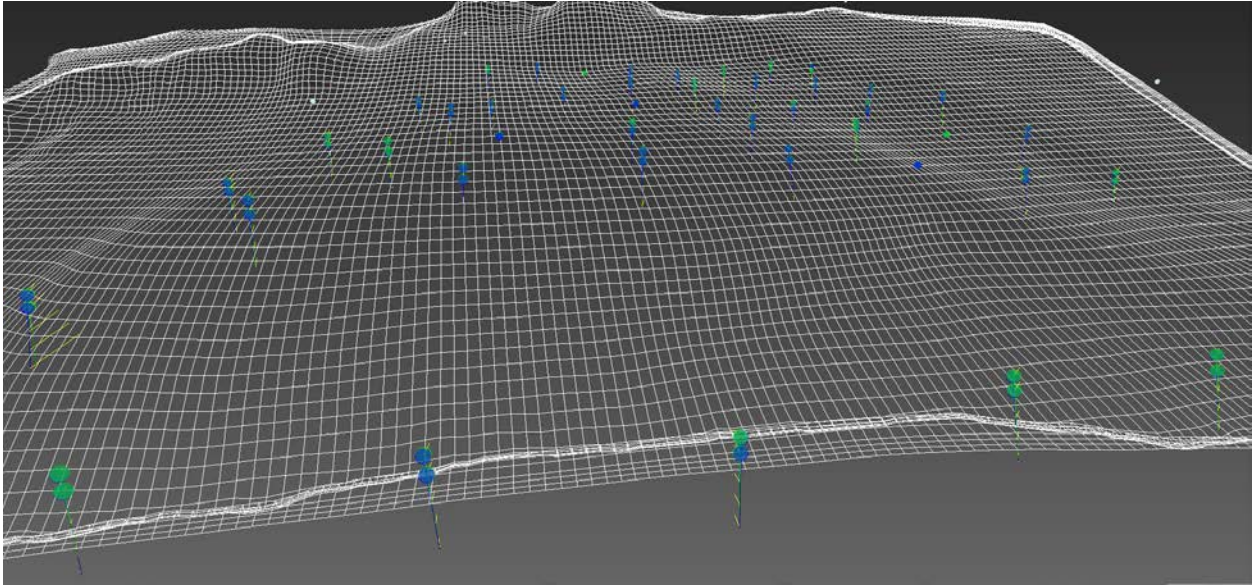
Figure 11: LIDAR scan of the position and movement of the balls on the slope. Green is the original positions, blue the displaced positions.

Figures 10 and 11 show the final layout of the balls. Comparison of the two scans revealed movement of the balls located outside the slide area equal to 6.0 mm in random directions (Table 1), whereas the balls located outside the slide are moved on average 16.7 mm in the downslope direction (Figure 12) (Table 2).
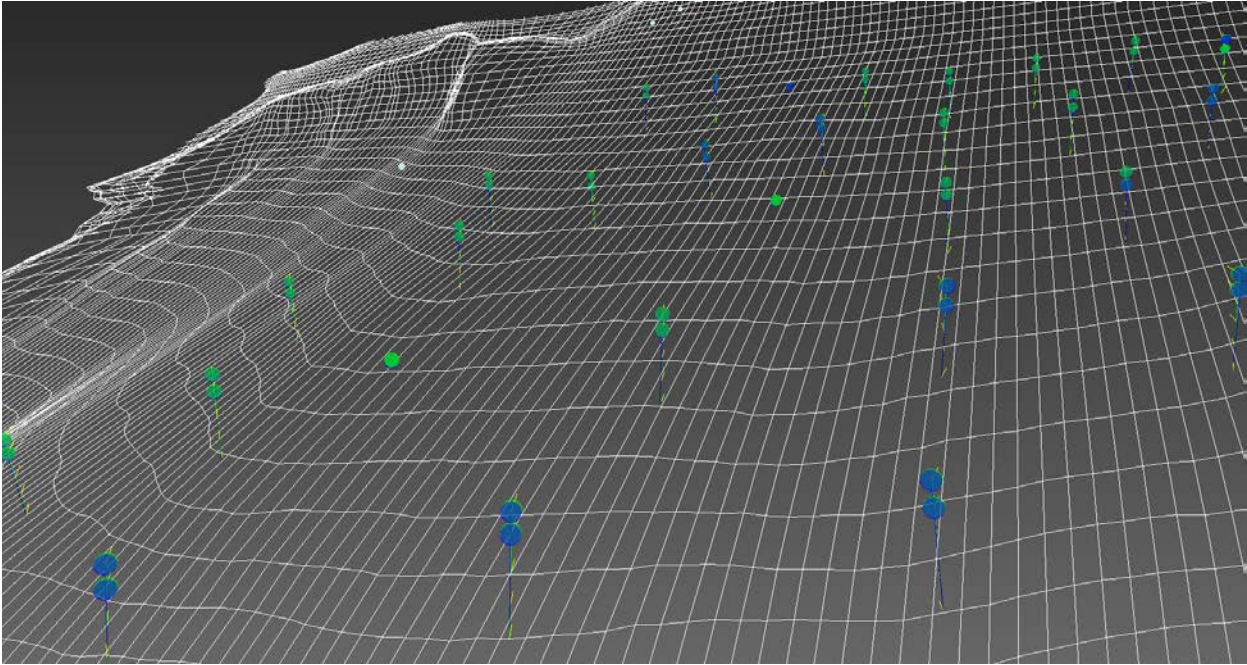
Figure 12: Downslope movement of the balls in the slide. Green is the original positions, blue the displaced positions

Table 1: Measured displacement of balls outside the slide area.

Ball number	Displacement in mm
1	2.74
2	4.31
3	10.32
4	2.89
5	3.04
104	5.86
105	12.97
106	5.89

Table 2: Measured displacement of balls inside the slide area.

Ball number	Displacement in mm	Ball number	Displacement in mm
7	14.96	55	42.8
8	45.34	56	13.73
9	25.79	57	16.68
10	25.66	58	16.15
11	26.99	59	18.74
12	21.47	60	11.12
13	21.75	61	10.87
14	15.31	62	11.87
15	15.72	63	12.23
16	13.88	64	13.22
17	12.4	65	11.95
18	12.06	66	13.63
19	14.48	67	14.48
20	21.98	68	9.66
21	20.86	70	17.91
22	14.76	71	20.13
23	14.81	72	12.28
24	14.6	73	12.36
25	14.6	74	11.85
26	17.02	75	11.18
27	15.35	76	13.97
28	14.04	77	13.54
29	15.94	80	22.98
30	20.28	81	26.82
31	21.51	83	14.29
32	16.72	84	13.61
33	18.04	85	12.63
34	15.09	86	13.32
38	15.94	87	13.68
39	16.28	88	12.9
41	12.44	89	13.5
42	14.45	90	13.23
43	15.43	91	13.03
44	18.09	92	21.41
45	19.38	93	24.27
46	14.88	94	12.03
47	13.65	95	12.89
49	14.75	96	13.47
50	17.94	97	14.54
51	20.05	98	12.92
52	14.29	99	12.68
53	13.31	100	17.2
54	35.71	101	17.68

6. Acknowledgements